

## **Review of the Most Applicable Regulator Collections to Control the Parallel Active Power Filter**

**Belkacem Gasmi<sup>1</sup>, Othmane Abdelkhalek<sup>2</sup>**

Smart Grids and Renewable Energies Lab, Department of Electrical Engineering,  
TAHRI Mohammed University, Bechar, Algeria

---

### **Article Info**

#### **Article history:**

Received Oct 17, 2017

Revised Dec 14, 2017

Accepted Dec 28, 2017

---

#### **Keyword:**

Fuzzy logic

HYSTERESIS

NSVPWM

Parallel Active Power Filter

(PAPF)

PWM

Regulator collections

SVPWM

---

### **ABSTRACT**

This work presents a study of the three-phase parallel active power filter and the various controllers used in its control. Moreover, in order to improve the quality of electrical energy, by making it conform to the new normative constraints, we have also been led to develop and apply advanced automation methods. In this framework, this paper reports of several regulatory structures: fuzzy logic, PWM, new space vector PWM (NSVPWM), space vector PWM (SVPWM), HYSTERESIS moreover, in order to produce a parallel active filter, a thorough study of experimental feasibility was carried out, taking into account the industrial constraints of the product both in its design and its application.

*Copyright © 2018 Institute of Advanced Engineering and Science.  
All rights reserved.*

---

#### **Corresponding Author:**

Belkacem Gasmi,

Smart Grids and Renewable Energies Lab,

Departement of Electrical and Engineering,

University Tahri Mohammed,

Street of Independence Bechar Algeria Bp 417.

Email: belkacemtube@gmail.com

---

## **1. INTRODUCTION**

Progressively, and in order to stem the increase in disturbance problems on power grids, increasingly stringent electrical quality standards will be imposed on suppliers and industrial consumers. Faced with these new regulations but also in response to the increasingly specific demand of electric power users, active compensators must adapt by making their structures and methods of regulation more complex. Especially since these solutions must be subject to the physical and technological limits inherent in active filtering devices[1,2].

Within the framework of this research problem, a paper has been initiated within Simulink in order to optimize the control performance of the active compensators while taking into account all the constraints and material limitations inherent in their structures. Thus, advanced studies have been carried out on the different types of regulator existing and on their feasibility in terms of digital implantation[3].

An industrial partnership has been added to this research in order to validate the experimental feasibility of our investigations. It was a research laboratory: Smart Grids & Renewable Energies Lab. (SGREL), University of Bechar Algeria, which wanted to develop an industrial prototype of parallel universal active filter capable of adapting and compensating as widely as possible all the current disturbances that could appear on the electrical network[4].

## 2. STRUCTURE OF PAPF SYSTEM

The active filter connected in parallel to the network, as shown in figure (1), is most often controlled as a current generator. It injects into the network disturbing currents equal to those absorbed by the polluting charge, but in phase opposition with them. The mains-side current is then sinusoidal. Thus, the objective of (PAPF) is to prevent disturbing (harmonic, reactive and unbalanced) currents produced by pollutant loads from circulating through the network impedance situated upstream of the connection point of the active filter[5-6].

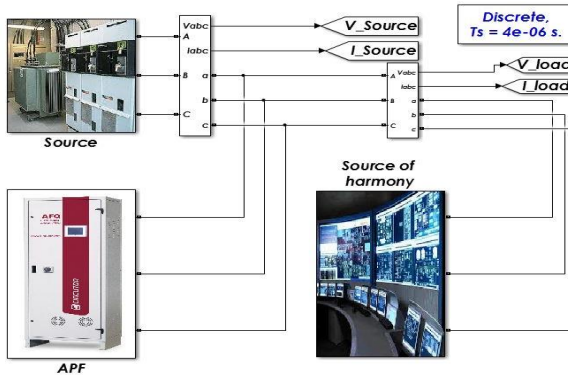


Figure 1. Block diagram of Basic Parallel Active Power Filter

From figure 1 the instantaneous currents can be written as equation 1.

$$i_s(t) = i_L(t) - i_C(t) \quad (1)$$

where:  $i_s(t)$  : source current,  $i_L(t)$  : current of load,  $i_C(t)$  : current of PAPF.

The source voltage is given by

$$v_s(t) = v_m \sin(\omega t) \quad (2)$$

where:  $v_s(t)$  : the source voltage,  $\omega$ : the pulsation.

if a nonlinear load is applied, then the load current will have a fundamental component, and the harmonic components can be represented as;

$$i_L(t) = \sum_{n=1}^{\infty} I_n \sin(n\omega t + \phi_n) \quad (3)$$

$$i_L(t) = I_1 \sin(\omega t + \phi_1) + \sum_{n=2}^{\infty} I_n \sin(n\omega t + \phi_n) \quad (4)$$

where:  $\phi$  : the phase difference between  $V_s(t)$  and  $i_L(t)$ .

Instantaneous load power can be given as

$$P_L(t) = v_s(t) \cdot i_L(t) \quad (5)$$

$$P_L(t) = V_m I_1 \sin^2(\omega t) \cos(\phi_1) + V_m I_1 \sin(\omega t) \cos(\omega t) \sin(\phi_1) + V_m \sin(\omega t) \sum_{n=2}^{\infty} I_n \sin(n\omega t + \phi_n) V_s(t) - i_L(t)$$

$$P_L(t) = P_f(t) + P_r(t) + P_h(t) \quad (6)$$

where:  $P_L(t)$ : the power of the load,  $P_f(t)$ : active power,  $P_r(t)$ : reactive power,  $P_h(t)$ : the deforming power.

from equation (6) real (Fundamental) power is drawn by the load

$$P_f(t) = V_m I_I \sin^2(wt) * \cos(\phi_I) = v_s(t) * i_s(t) \quad (7)$$

from equation (7) the source current supplied by the source, after compensation

$$i_s(t) = \frac{P_f(t)}{v_s(t)} = + I_I \cos(\phi_I) \sin(wt) = I_{sm} \sin(wt) \quad (8)$$

Hence, total peak current supplied by the source

$$I_{sp}(t) = I_{sm} + I_{sL} \quad (9)$$

where:  $I_{sp}(t)$ : total peak current supplied by the source,  $I_{sL}(t)$ : the peak current absorbed by the load.

The active filter must provide the following compensation current, as shown in equation (9).

It  $i_c(t) = i_L(t) - i_s(t)$  is necessary to calculate  $i_s(t)$ . The purpose of active filtering is the generation of harmonic currents of the same amplitude but in phase opposition with those absorbed by the load. Thus, the current absorbed to the network will be sinusoidal. It is necessary to precisely identify the harmonic currents of the pollutant load. The reference source currents  $I_{sp}$  after compensation can be given as

$$i_{sb}^* = I_{sp} \sin(wt) \quad (10)$$

$$i_{sb}^* = I_{sp} \sin(wt - 120^\circ) \quad (11)$$

$$i_{sb}^* = I_{sp} \sin(wt + 120^\circ) \quad (12)$$

where:  $i_{sb}^*$ : the reference source currents after compensation.

The energy storage on the DC side is often done by a capacitive storage system represented by a capacitor  $C_{dc}$  which plays the role of a DC voltage source  $V_{dc}$ . The choice of the storage system parameters ( $V_{dc}$  et  $C_{dc}$ ) affects the dynamics and compensation quality of the active parallel filter. Indeed, a high voltage  $V_{dc}$  improves the dynamics of the active filter. Moreover, the undulations of the DC voltage  $V_{dc}$ , caused by the currents generated by the active filter and limited by the choice of  $C_{dc}$ , can degrade the compensation quality of the parallel active filter. These fluctuations are all the more important as the amplitude of the filter current is large and its frequency is low. The DC voltage  $V_{dc}$  must be high enough to improve the controllability of the active filter while respecting the threshold voltage of switches. By respecting this compromise, a DC voltage is chosen:  $V_{dc} = 800$  V.

## 2.1. Harmonic currents control using fuzzy logic

One of the main applications is the control of systems for which there is no specific model (Figure 2). The fuzzy controller receives as input an observation of the system (for example the error with respect to the set point) and deduces a command to be applied to the system, according to a decision table (rules). The quantities manipulated by the controller are fuzzy sets (eg large, medium, small), which necessitates a conversion of the numerical values as input, this is the 'fuzzification'. Depending on these fuzzy variables and decision rules, the controller calculates the fuzzy value of the command, this is the inference. It is then necessary to convert this variable into a numerical value, that is defuzzification, the rules model the knowledge of an expert or the behavior of another controller capable of regulating the system. The detailed study of these three parts is necessary to determine the structure of the controller that will best answer the problem posed[7].

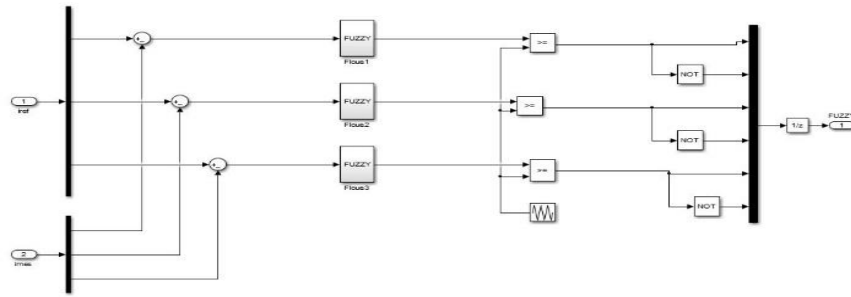


Figure 2. MATLAB Simulink model of fuzzy logic controller

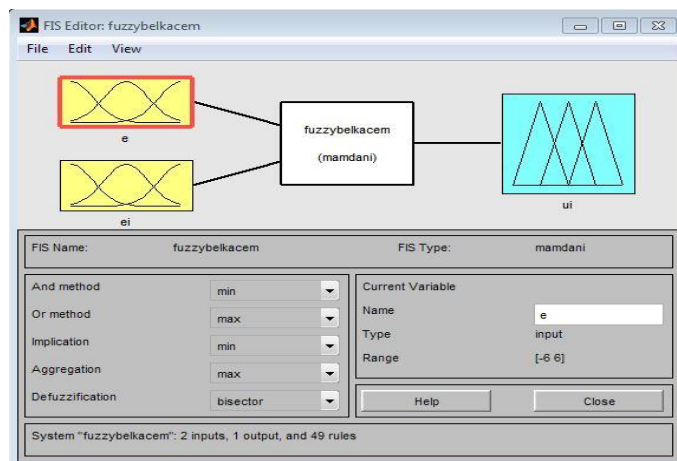


Figure 3. The membership function of input and output



Figure 4. Rules of fuzzy logic controller

## 2.2. Harmonic currents control using PWM

The pulse width modulation (PWM) control technique solves the problem of controlling the switching frequency by operating with a fixed frequency easy to filter downstream of the inverter [8]. The simplest and best known pulse width modulation is undoubtedly the natural sampling MLI. This control technique first uses a regulator which determines the reference voltage of the inverter from the difference between the measured current and its reference. This voltage is then compared with a saw tooth signal (high frequency carrier fixing the switching frequency). The output of the comparator supplies the control command of the switches. The general block diagram of control currents is illustrated in Figure 2[9].

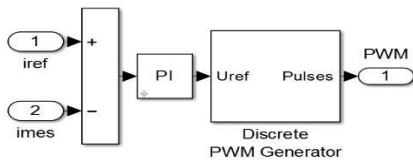


Figure 5. PWM synoptic block diagram of currents control

### 2.3. Harmonic currents control using SVPWM

The SVPWM method is widely used in inverter control, it can increase the maximum value of the inverter output voltage with a reduced harmonic distortion rate compared to those obtained by the sinusoidal PWM method[10]. The goal of all modulation strategies is to reduce switching losses and harmonics, and to provide accurate control. The SVPWM command consists of placing the control vector in the two - use of the Clark transformation. The coding of the possible switches of the switches can be carried out on three states eight possible vectors of which two are zero ( $V_0$  and  $V_7$ )[11].The relationship between the switching variable vector  $[a,b,c]^T$  and line-to-line voltage vector  $[V_{ab}, V_{bc}, V_{ca}]$  is given by (13) in the following:

$$\begin{bmatrix} V_{ab} \\ V_{bc} \\ V_{ca} \end{bmatrix} = V_{dc} \begin{bmatrix} 1 & -1 & 0 \\ 0 & 1 & -1 \\ -1 & 0 & 1 \end{bmatrix} \begin{bmatrix} a \\ b \\ c \end{bmatrix} \quad (13)$$

Also, the relationship between the switching variable vector  $[a,b,c]^T$  and the phase voltage vector  $[V_{ab}, V_{bc}, V_{ca}]$  can be expressed below.

$$\begin{bmatrix} V_{an} \\ V_{bn} \\ V_{cn} \end{bmatrix} = \frac{V_{dc}}{3} \begin{bmatrix} 2 & -1 & -1 \\ -1 & 2 & -1 \\ -1 & -1 & 2 \end{bmatrix} \begin{bmatrix} a \\ b \\ c \end{bmatrix} \quad (14)$$

where :  $V_{an}$ ,  $V_{bn}$ ,  $V_{cn}$  : simple voltages.

the detail of eight voltage vectors is presented in Table 1

Table 1. Switching vectors, phase voltages and output line to line voltages

Voltage vectors	Switching vectors			Line to neutral voltage			Line to line voltage		
	a	b	c	$V_{an}$	$V_{bn}$	$V_{cn}$	$V_{ab}$	$V_{bc}$	$V_{ca}$
$V_0$	0	0	0	0	0	0	0	0	0
$V_1$	1	0	0	$\frac{2}{3}$	$-\frac{1}{3}$	$-\frac{1}{3}$	1	0	-1
$V_2$	1	1	0	$\frac{1}{3}$	$-\frac{1}{3}$	$-\frac{2}{3}$	0	1	-1
$V_3$	0	1	0	$-\frac{1}{3}$	$\frac{2}{3}$	$-\frac{1}{3}$	-1	1	0
$V_4$	0	1	1	$-\frac{2}{3}$	$\frac{1}{3}$	$\frac{1}{3}$	-1	0	1
$V_5$	0	0	1	$-\frac{1}{3}$	$-\frac{1}{3}$	$\frac{2}{3}$	0	-1	1
$V_6$	1	0	1	$\frac{1}{3}$	$-\frac{2}{3}$	$\frac{1}{3}$	1	-1	0
$V_7$	1	1	1	0	0	0	0	0	0

Figure 6 shows the block diagram of proposed active filter control method implemented using SVPWM in MATLAB /Simulink.

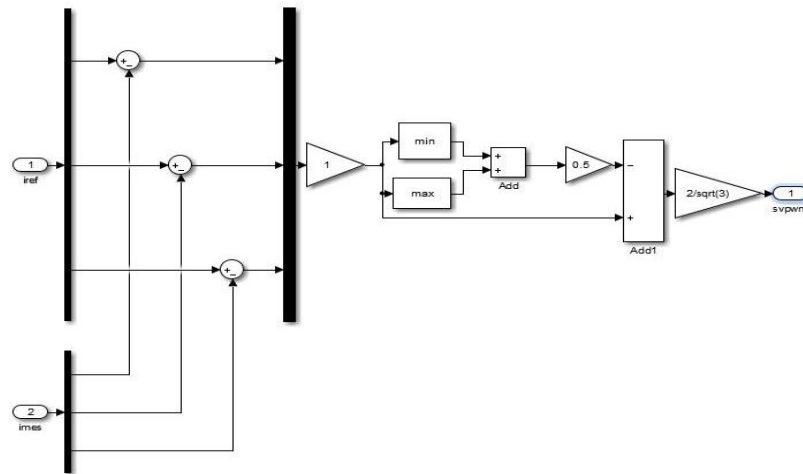


Figure 6. SVPWM synoptic block diagram of currents control

#### 2.4. Harmonic currents control using hysteresis

Conventional hysteresis control is very commonly used due to its ease of use and robustness. In fact, this strategy ensures satisfactory control of the current without requiring a thorough knowledge of the model of the system to be controlled or of its parameters. The principle of first establishing the error signal, the difference between the reference current  $i_{ref}$  and the current produced by the inverter  $i_f$ , is shown in figure (7). This error is then compared with a template called a hysteresis band in order to fix the control commands of the switches. However, this control has a major disadvantage: it does not make it possible to control the switching frequency of the semiconductors, hence the presence of a large number of harmonics in the generated currents[12,13].

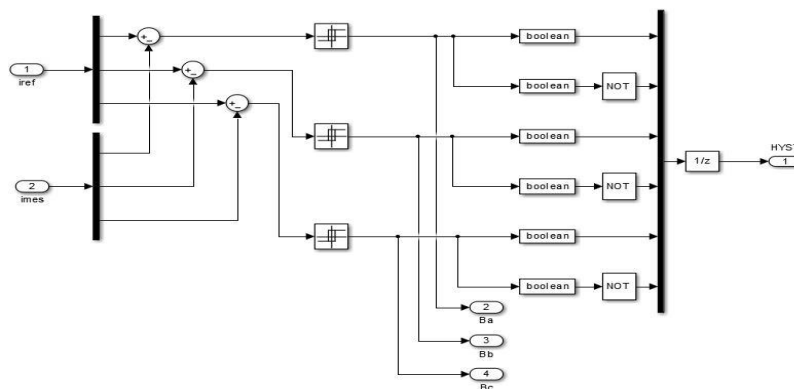


Figure 7. Hysteresis synoptic block diagram of currents control

The switching logic is formulated as follows:

If  $i_{ca} < (i^*c_a - HB)$  upper switch is OFF and lower switch is ON for leg "a" (SA = 1).

If  $i_{ca} > (i^*c_a + HB)$  upper switch is ON and lower switch is OFF for leg "a" (SA = 0).

#### 2.5. Harmonic currents control using NSVPWM (proposed method)

The strategy proposed in this paper is an NSVPWM with hysteresis that can be implemented by the

following figure:

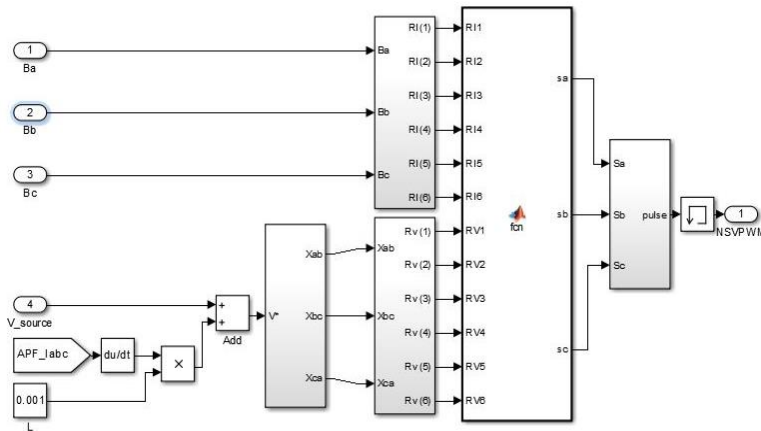


Figure 8. NVPWM synoptic block diagram of currents control

From Figure 8,  $V^*$  can be calculated as follows:

$$\begin{aligned} \mathbf{V}^* &= \begin{vmatrix} V_a^* \\ V_b^* \\ V_c^* \end{vmatrix} = \mathbf{U}_s + \mathbf{U}_f \\ \mathbf{U}_f &= L_f \frac{du}{dt} \times \mathbf{I}_f \end{aligned} \quad (15)$$

where:  $V^*$  : the reference voltage,  $U_f$  : source voltage,  $U_f, L_f, I_f$  : respectively the voltage, inductance, current of PAPF.

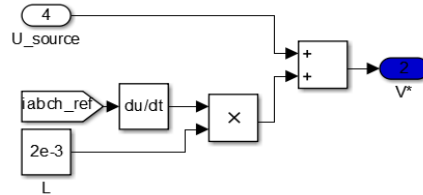


Figure 9. The output voltage  $V^*$ .

Determine  $V_{ab}, V_{bc}, V_{ca}$  and  $X_{ab}, X_{bc}, X_{ca}$

$$\begin{aligned} V_{ab} &= V_a^* - V_b^* \\ V_{bc} &= V_b^* - V_c^* \\ V_{ca} &= V_c^* - V \\ X_{ab} &= \begin{cases} 1 & V_{ab} \dots X_{bc} \\ 0 & V_{bc} \dots X_{ca} \\ 0 & V_{ca} \end{cases} \end{aligned} \quad (16)$$

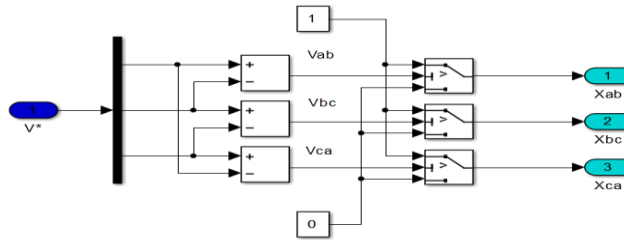


Figure 10. The outputs : Xab,Xbc and Xca

Determine RV(1), RV(2), RV(3), RV(4), RV(5) and RV(6)From Figure 6, RV(1), RV(2), RV(3),RV(4), RV(5) and RV(6) can be determined as follows:

$$\begin{aligned}
 RV(1) &= \overline{X_{ab}} + X_{bc} + \overline{X_{ca}} \\
 RV(2) &= \overline{X_{ab}} + X_{bc} + X_{ca} \\
 RV(3) &= \overline{X_{ab}} + \overline{X_{bc}} + X_{ca} \\
 RV(4) &= \overline{X_{ab}} + \overline{X_{bc}} + X_{ca} \\
 RV(5) &= X_{ab} + \overline{X_{bc}} + \overline{X_{ca}} \\
 RV(6) &= X_{ab} + \overline{X_{bc}} + X_{ca}
 \end{aligned} \tag{17}$$

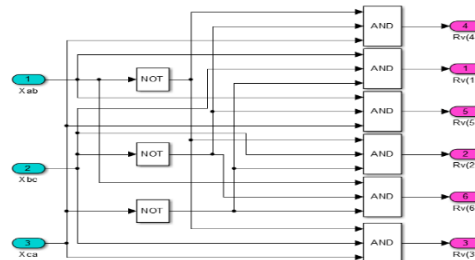


Figure 11. The outputs: RV(1), RV(2), RV(3), RV(4), RV(5) and RV(6) generating of the inverter switching pulses Figure 12 shows the NSVPWM pulses to attack the gates of AP

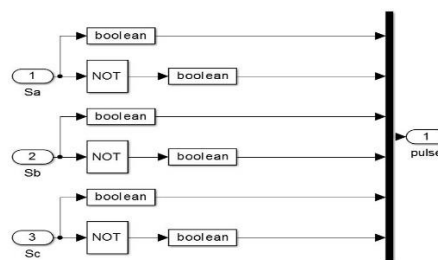


Figure 12. The output pulses to attack the gates of multilevel inverters

### 3. MATLAB BASED SIMULATION

The simulated system is shown in figure 13. It is composed of a power supply network, a rectifier bridge and an active current structure filter. The rectifier flowing on an R-L load plays the role of the polluting load. The active filter consists of an inverter with six switches and a perfect current source. The inverter bridge switches are formed by IGBTs (with antiparallel diodes) in series with diodes.

The simulation results for the five control techniques make it possible to demonstrate the performance of each of the five controllers. Figures 13 to 17 illustrate the response of the three-phase shunt

filter in steady-state and transient conditions: we present in particular the voltage of the source  $V_s$ , the current of the source  $i_s$ , the reference current  $i_{ref}$ , the current consumed by the load  $i_L$ , the voltage across the terminals of capacitor  $V_{dc}$ , the harmonic distortion rate THD of the line current and the current of the load. The simulation parameters used in the different control techniques are presented in Table 2.

Table 2. The parameters of the simulated system

Total Line impedance	x/r = 10
Non-linear load(rectifier with $R_{dc}L_{dc}$ )	$R_{dc}= 10/3 \Omega$ , $L_{dc}= 60e-3 \Omega$
Coupling Impedance	$L_f=0.001mH$
Dc bus voltage	410V
Max switching frequency	12kHz
Hysteresis band(Hb)	0.5 A
Dead time	8μs
Line frequency	50Hz
Phase-to-phase rms voltage	380V

#### 4. RESULTS AND DISCUSSION

The performance of the parallel active filter with the five controllers is given in figure 14 at figure 17. The three-phase sinusoidal supply voltage of 380v, 50hz is applied to the load non-linear injecting harmonics into the system. The charging current patterns: 14,15,16,17 and 18 (fuzzy logic (subschema (6,5,16)), PWM (subschema (6,5,17), NSVPWM, 5,18 ), SVPWM (sub-plot (6,5,19), HYSTERESIS (sub-plot (6,5,20)) in THD is set at 26,95%. Shunt current reference figures: 14 sub- (6.5, 26, 15 sub-plots (6.5,27), 16 sub-plots (6.5,28), 17 sub-plots (6.5,29) and 18 sub-plots, 5,30) so that the harmonic content of the supply current is reduced. When the reference voltage capacitor is charged, the charging current is drawn by  $V_{dc}$  from the power supply. By using the five controllers, it is charged to a required value and maintained constant. The harmonics of the load current are compensated by the shunt inverter, the DC side of the inverter before compensating (6,5,21), 15 subtotals (6, 5,22), 16 subtotals (6,5,23), 17 subtotals (6,5,24) and 18 subtotals (6,5,25) and after compensation of the source current is represented in the figures: 14 sub-frames (6,5,11), 15 sub-paths (6,5,12), sub-paths (6,5,13), 17 sub-frames 18 sub-plots (6,5,15). The performance of the PAPF based on the five current controllers in terms of harmonic elimination is very satisfactory.

In this comparison, it is found that the controller FUZZY, SVPWM and HYSTERESIS do not effectively reduce the harmonic current of the source to the initial conditions and also when there is disturbance of the load. On the other hand, the PWM and NSVPWM controllers more efficiently reduce the harmonic current of the source than the precise controllers. In addition, it controls the DC link with less distortion.

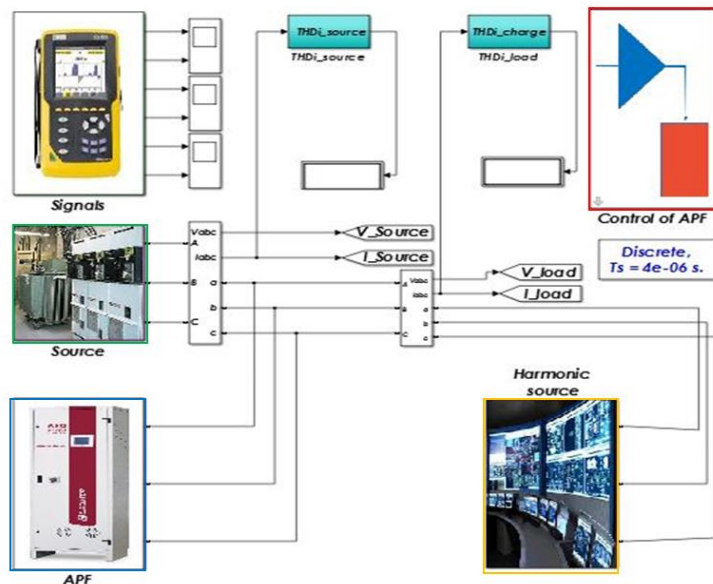


Figure13. Main block of proposed control scheme with PAPF under MATLAB

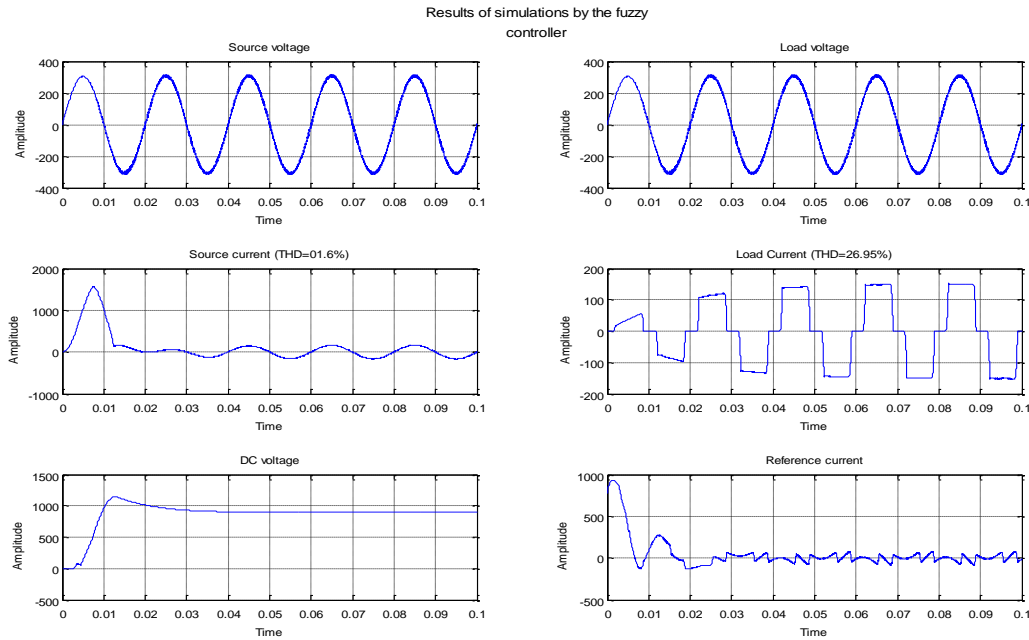


Figure 14. Performance of the parallel active power filter with the FUZZY LOGIC controller

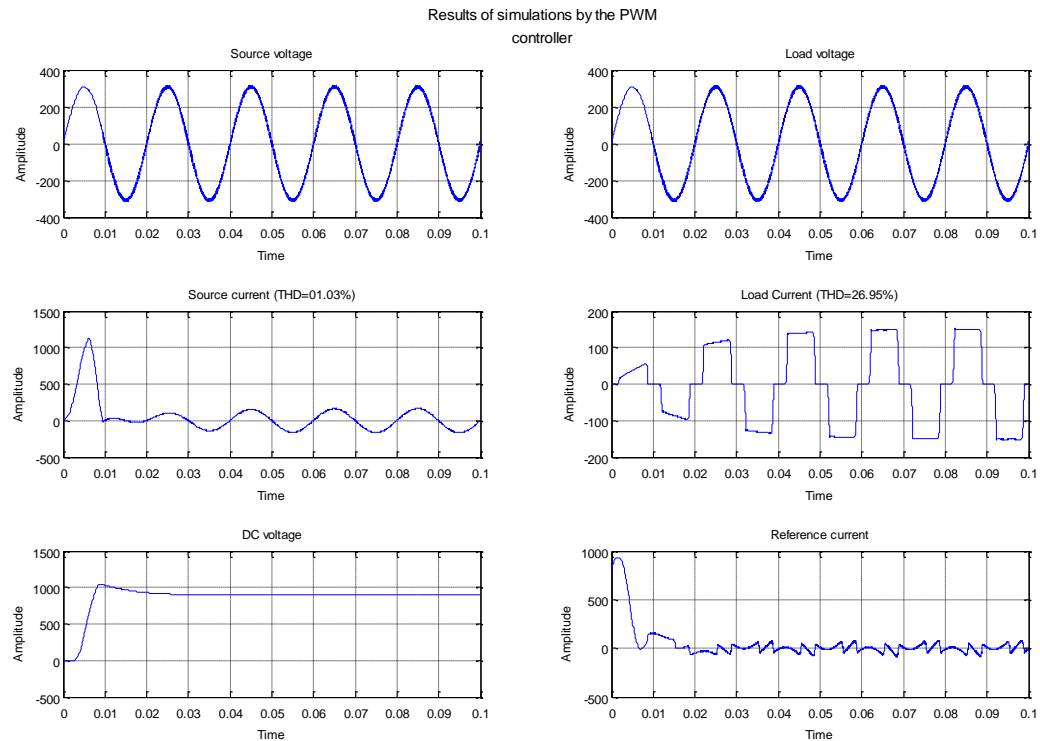


Figure 15. Performance of the parallel active power filter with the PWM controller

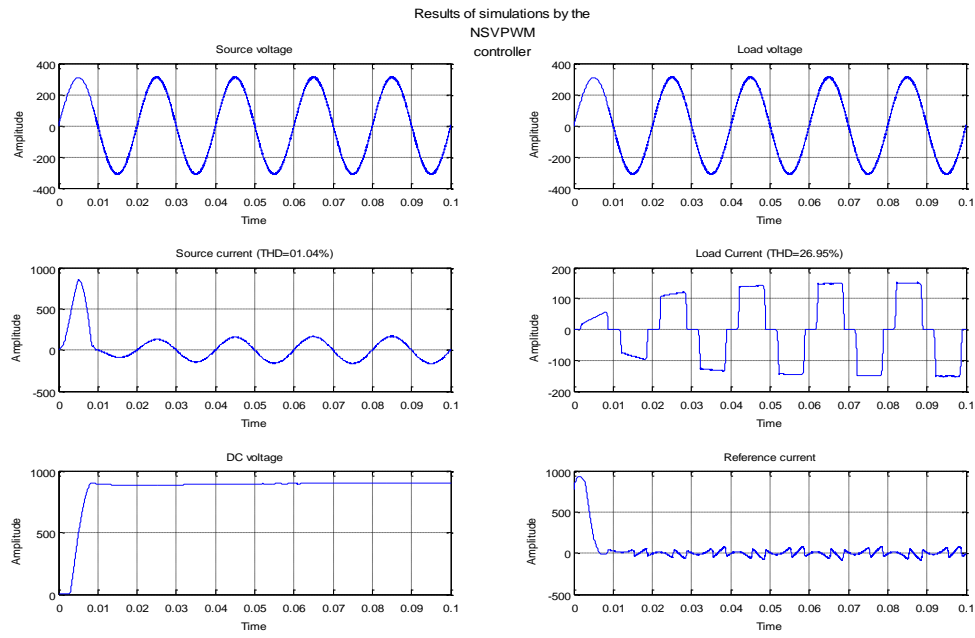


Figure 16. Performance of the parallel active power filter with the NSVPWM controller

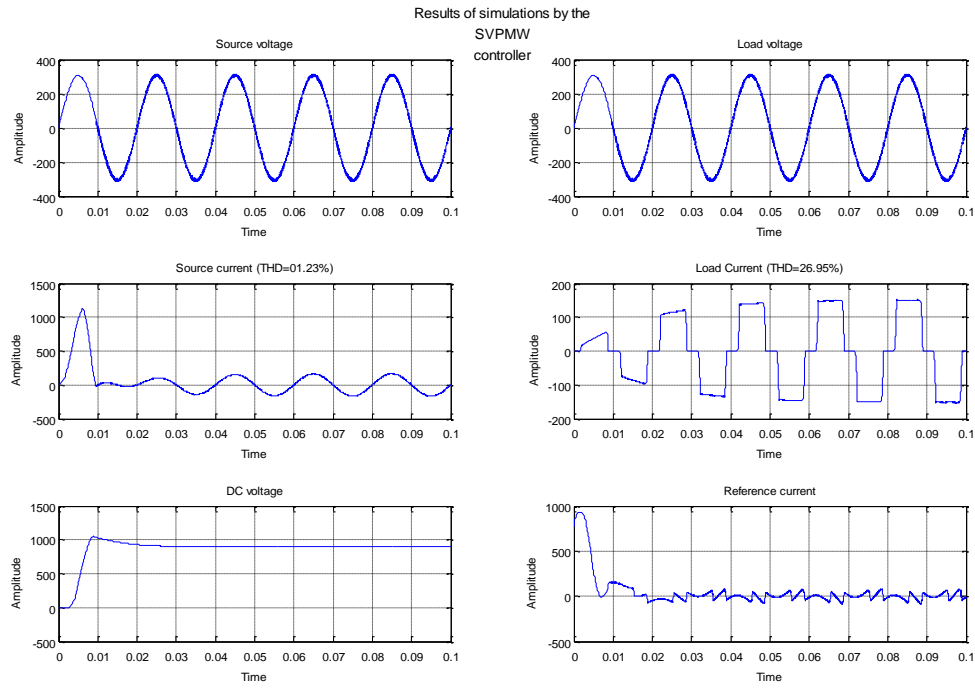


Figure 17. Performance of the parallel active power filter with the SVPWM controller

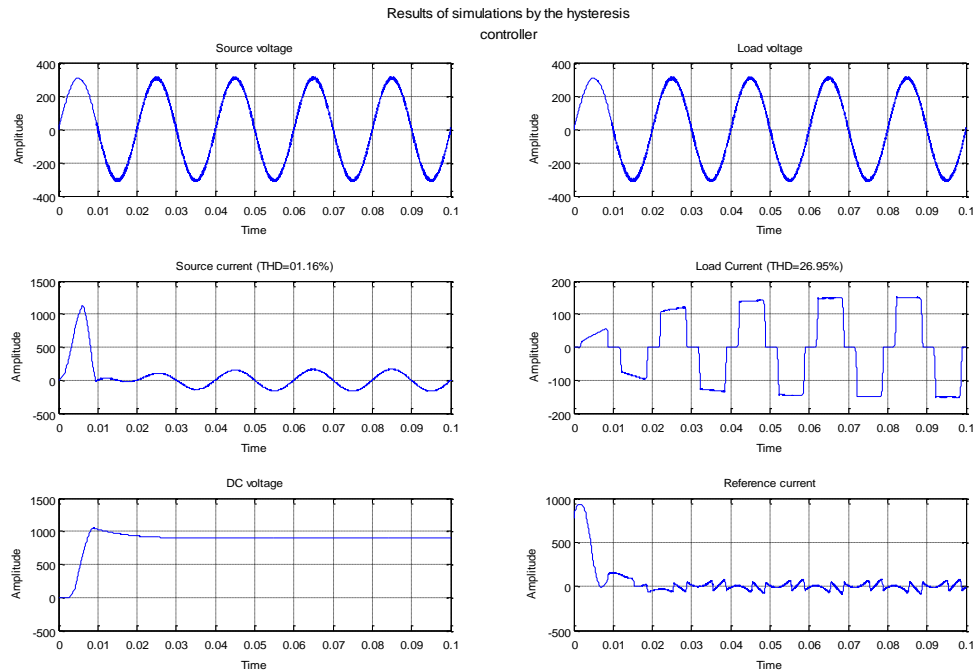


Figure 18. Performance of the parallel active power filter with the HYSTERESES controller

Table 3. Performance of different controllers to the current control within the PAPF

Five controllers	Response time (dynamic) (ms)	Static Error (%)
fuzzy logic	32	8.04
PWM	37	13.37
NSVPWM	20	6.2
SVPWM	35	11.23
HYSTERESIS	42	14.58

To accurately reflect the performance of different types of controllers used, Table 3 evaluates according to the following criteria:

1. the response time (dynamic)
2. the static error

Table 3 gives the results for each type of controller used. In the case of a large pollution of the load, we see that the controller hysteresis gives a good compensation in terms of error of the current source side. The NVSPWM controller gives a better result than the other controllers, and on the other hand it is found that the error between the reference current and the current injected by the NVSPWM controller is kept below 6.5% and follow its reference quickly after a half wave period (13ms) against 14.58% with a hysteresis controller.

## 5. CONCLUSION

The performance of the PAPF depends mainly on the accuracy and speed of the reference signals. It has been observed that the power conditioner should have a stable filter current for better compensation of load harmonics and voltage failures. To improve its response time, we propose the FUZZY logic, PWM, NSVPWM, SVPWM and HYSTERESIS controllers, and their performances are analysed using the MATLAB simulation. The PWM and NSVPWM controllers are best suited to reduce the harmonic current of the source compared to the FUZZY, SVPWM and HYSTERESIS controller. In addition, they control the DC link with less distortion than other controllers.

**REFERENCES**

- [1] S.M.Mahi., O. Abdelkhalek., B. Kadri., "SAPF using Xilinx SysGen by PQ method based on CIC filter". in *Electrotehnica, Electronica, Automatica (EEA)*, 2017, vol. 65, no. 2, pp. 120-125, ISSN 1582-5175.
- [2] O. Abdelkhalek., A.Kechich., C.Benachiba., "Comparative Study between Two Topologies of an UPQC Six-Leg and an UPQC Seven-Leg". in *Electrotehnica, Electronica, Automatica (EEA)*, 2014, vol. 62, no. 4, pp. 70-78, ISSN 1582-5175.
- [3] S.Khalid., "Performance Evaluation of GA optimized Shunt Active Power Filter for Constant Frequency Aircraft Power System", in *Indonesian Journal of Electrical Engineering and Informatics (IJEI)*, 2016, Vol.4, No.2, pp. 112-119.
- [4] M. Tamilvani., K. Nithya., M. Srinivasan., "Harmonic Reduction in Variable Frequency Drives Using Active Power Filter", in *TELKOMNIKA Indonesian Journal of Electrical Engineering (TELKOMNIKA)*, 2014, Vol. 12, No. 8, pp. 5758- 5765.
- [5] K.Hachani., D.Mahi., A.Kouzou., "Shunt Active Power Filtering based on the p-q Theory Control", in *Electrotehnica, Electronica, Automatica (EEA)*, 2017, vol. 65, no. 3, pp. 85-89, ISSN 1582-5175.
- [6] S.Chennai., " Efficient Control Scheme for Five-Level Shunt Active Power Filter to enhance the Power Quality", in *Electrotehnica, Electronica, Automatica (EEA)*, 2016, vol. 64, no. 2, pp. 124-129, ISSN 1582-5175.
- [7] R.Belaidi., R.Haddouche., "Three-phase four-Wire Active Power Filter fed by PV System using Fuzzy MPPT Controller", in *Electrotehnica, Electronica, Automatica (EEA)*, 2017, vol. 65, no. 3, pp. 17-25, ISSN 1582-5175.
- [8] S.Chennai., "Steady and Dynamic Performances Evaluation of Three-Level Shunt Active Power Filter for Power Quality Improvement", in *Electrotehnica, Electronica, Automatica (EEA)*, 2016, vol. 64, no. 4, pp. 75-82, ISSN 1582-5175.
- [9] Y.R.Badu., "Distributed Generation Inverter as APF in Dual APF DGInterfacing Scheme", in *International Journal of Power Electronics and Drive System (IJPEDS)*, 2017, vol. 8, no. 3, pp. 1441-1454.
- [10] K.S.Gaeid., M.T.Hamood., "Distributed Unified Power Quality Conditioner Model Based with Seriesand Shunt Filters", in *International Journal of Power Electronics and Drive System (IJPEDS)*, 2017, vol. 7, no. 3, pp. 743-758.
- [11] C. Subramani., " Space Vector and Sinusoidal Pulse Width Modulation of QuasiZ-Source Inverter for Photovoltaic System", in *International Journal of Power Electronics and Drive System (IJPEDS)*, 2016, vol. 7, no. 3, pp. 601-609.
- [12] S. Ojha., A.K.Pandey., "Close Loop V/F Control of Voltage Source Inverter usingSinusoidal PWM, Third Harmonic Injection PWM and SpaceVector PWM Method for Induction Motor", in *International Journal of Power Electronics and Drive System (IJPEDS)*, 2016, vol. 7, no. 1, pp. 217-224.
- [13] T.R.Chowdhury., B. Nayak., "Modeling and Analysis of a Novel Adaptive Hysteresis Band Controller for Boost and Buck Converter", in *International Journal of Power Electronics and Drive System (IJPEDS)*, 2017, vol. 8, no. 1, pp. 305-315.

**ACKNOWLEDGMENT**

Acknowledgment should be given to those who help me in this work: my Prof Othmane Abdelkhalaik.

**BIOGRAPHIES OF AUTHORS**

Belkacem Gasmi was born in Ain sefra (Algeria), on Juin 06, 1984. He received the Magister degree from Bechar University, Bechar, Algeria, In 2008 and 2011, respectively. Where he has been working toward the Ph.D. degree in the Department of Electric and Electronics Engineering since september 2011. His research interests concern: power electronics, Power Quality, and Power Systems FACTS. Her research interests are are: His research interests concern: power electronics, Power Quality, and Power Systems FACTS.



Othmane Abdelkhalek was born in Bechar (Algeria), on August 22, 1976. He graduated in the University of Bechar, Department of Electrical Engineering (Algeria), in 2001. He received the PhD degree in electrical engineering from the University of Bechar (Algeria), in 2010. He is an Assistant Professor at the University of Bechar.His research interests concern: power electronics, Power Quality, artificial intelligence and Power Systems.